Population model of hippocampal pyramidal neurons, linking a refractory density approach to conductance-based neurons

Anton V. Chizhov* and Lyle J. Graham

Laboratory of Neurophysics and Physiology, UMR 8119 CNRS, University Paris–5, 45 rue des Saint-Peres, 75006, Paris, France

(Received 19 May 2006; revised manuscript received 19 October 2006; published 26 January 2007)

We propose a macroscopic approach toward realistic simulations of the population activity of hippocampal pyramidal neurons, based on the known refractory density equation with a different hazard function and on a different single-neuron threshold model. The threshold model is a conductance-based model taking into account adaptation-providing currents, which is reduced by omitting the fast sodium current and instead using an explicit threshold criterion for action potential events. Compared to the full pyramidal neuron model, the threshold model well approximates spike-time moments, postspike refractory states, and postsynaptic current integration. The dynamics of a neural population continuum are described by a set of one-dimensional partial differential equations in terms of the distributions of the refractory density (where the refractory state is defined by the time elapsed since the last action potential), the membrane potential, and the gating variables of the voltage-dependent channels, across the entire population. As the source term in the density equation, the probability density of firing, or hazard function, is derived from the Fokker-Planck (FP) equation, assuming that a single neuron is governed by a deterministic average-across-population input and a noise term. A self-similar solution of the FP equation in the subthreshold regime is obtained. Responses of the ensemble to stimulation by a current step and oscillating current are simulated and compared with individual neuron simulations. An example of interictal-like activity of a population of all-to-all connected excitatory neurons is presented.

DOI: 10.1103/PhysRevE.75.011924 PACS number(s): 87.19.La, 87.18.Sn, 87.19.Nn, 05.10.Gg

I. INTRODUCTION

Individual cortical neurons operate within the background activity of neuron populations occupying large areas of the cortex. Relative to the single-cell activity, this background activity is macroscopic, and therefore calls for independent approaches for its mathematical description. Whereas detailed single-neuron conductance-based models are well developed, there is no generally accepted derivation of a conductance-based macroscopic model of neuronal ensemble activity. Our approach considering a neural ensemble as a continuum in a state parameter space is based on the ideas and methods introduced in [1–3] and reviewed in [4]. The implementation of the theory based on the notion of a probability density function for a reduced and experimentally constrained single-neuron conductance-based model has been recently proposed in [5]. However, two important additional details are presented here, completing the generalization of the approach for a population of adaptive neurons, mainly pyramidal-like cells. These are the description of slow ionic currents and the extension of the hazard-function approximation to the range of subthreshold stimulation.

Population models of the firing rate type [6–10] were proposed to describe an infinite number of similar neurons as a continuum. Strictly, these methods are valid only for quasistationary states of ensemble activity, and only their modification with the help of *ad hoc* parameter fitting can provide good descriptions of transient regimes. One example is given in [8], where second-order filtering is used for the current that takes part in the basic dependence between firing rate and stimulus current. Another approach [10] is to separate steady and nonstationary firing regimes. Applying the rate-current dependence to the former regime and treating the latter as a superthreshold regime of abrupt excitation, one can get a rough approximation of the firing rate. However, such approaches either do not allow a precise approximation or work only in a limited range of stimulation parameters.

We apply the probability density approach (PDA) which, in contrast to the firing-rate models, can take into account the relaxation properties of neurons and thereby correctly calculate the firing rate in nonstationary dynamical regimes [2]. The PDA describes the evolution of a neuronal continuum in the phase space of a specific choice of neuronal state variables. In general, if we consider a conductance-based-type model of a single neuron, the state variables include the membrane potential and those describing the ionic current conductances. However, the large number of associated parameters for the conductance-based model necessarily complicates the equations for the ensemble dynamics. This is a major reason that many approaches consider only one state variable, the membrane potential, governed by the integrate-and-fire or the spike response model (e.g., [11]). Nevertheless, the membrane potential is only a weak predictor of the neuron's complete state, primarily because neurons with different refractory states can have the same potential. On the other hand, the time elapsed since the last action potential approximates the refractory state quite well. This relationship motivates a refractory density approach ([2,4]), which considers the evolution of a neuronal density distribution in the space of a single parameter, the time elapsed since the last spike, as a particular case of the probability density approach.

*Permanent address: A.F. Ioffe Physico-Technical Institute of RAS, 26 Politekhnicheskaya str., 194021, St.-Petersburg, Russia. Electronic address: Anton.Chizhov@mail.ioffe.ru

The key element of the present work is that of implanting a conductance-based neuron model into the probability density approach. To this end, following our previous work devoted to an interneuron population [5], we first develop a threshold version of the experimentally constrained conductance-based model, and then derive the appropriate system of equations of the refractory density approach (RDA) for this model.

The threshold model is obtained in Sec. II A by omitting the fast sodium current from the conductance-based model, and in its place introducing a threshold criterion that depends on the derivative of the membrane potential. The corresponding membrane potential is referred to as the averaged subthreshold potential over the neurons of a given population, under the assumption that the input current is equal for all neurons. Advantages of the model in comparison with the integrate-and-fire and spike response models are outlined in this section and in Sec. IV. The approximating formulas for the ionic currents are given in Appendix A. The approximation of the threshold as a function of the potential slope in the present model is obtained by comparing the solutions from both the biophysically detailed and reduced single-neuron models in Sec. II B.

In Sec. II C we write the equations of the RDA. For a large population of similar neurons we form a probability density that represents the distribution of neurons across all possible states. The state variables of a neuron are assumed to be dependent on only one parameter, which is the time elapsed since the last spike. This parametrization reduces the dimension of the phase space of neural states, yielding a set of one-dimensional partial differential equations. We calculate the membrane potential and the gating variables of ionic currents, along with the refractory density, by means of the threshold conductance-based model mentioned above; and these serve to define the term governing neural excitation in the RDA, referred to in [4] as the hazard function.

The differences in intrinsic properties between neurons within the given population, as well as fluctuations of any stochastic currents affecting the neurons, are taken into account by the hazard function. In Appendix B we derive the hazard function and show that it approximates well the firing probability of a neuron fluctuating due to noise near the mean state of the population for any regime of neuron stimulation. The resulting hazard function as the source term in the RDA is introduced in Sec. II C, which completes the composition of the full system of equations governing a single neural population.

In Sec. III we present the results of single-population simulations and comparison with simulations of an ensemble of noninteracting neurons. We discuss the results in Sec. IV.

II. GOVERNING EQUATIONS

Our implementation of the population density approach is based on a threshold model constructed from the conductance-based single-neuron model. Although the approach could be generalized or reduced to other neuron models (see [3,11,4]), the population model based on the proposed threshold neuron model is low dimensional, computationally efficient, biophysically meaningful, and matched to experiments. Based on the threshold neuron, we then make the main assumption that the state variables of the neuron are parametrized by a single parameter, the time elapsed since the last spike, which in turn allows the one-dimensional population density description.

A. Single-neuron model

A precise model of a hippocampal pyramidal cell can be found in [12]. Here we use a reduced version of the model, considering a one-compartment neuron with voltage-dependent sodium and potassium currents as well as an afterhyperpolarization (AHP) current which describes the cumulative activity of calcium-dependent potassium currents. Thus the membrane potential $V(t)$ is governed by the equation (in conventional notation)

$$C\frac{dV}{dt} = -I_{\mathrm{Na}} - I_{DR} - I_A - I_M - I_{\mathrm{H}} - I_L - I_{AHP} - I_a, \quad (1)$$

where I_a is the applied current, I_L is the linear leak current, and the membrane capacitance $C=0.37$ nF. The approximations of the current kinetics for the sodium current I_{Na}, the voltage-dependent potassium currents responsible for spike repolarization, I_{DR} and I_A, the voltage-dependent potassium current that contributes to spike frequency adaptation, I_M, and the voltage-dependent cation current I_{H}, are adapted from [12]; the approximation for the voltage and calcium-dependent potassium current that also contributes to spike frequency adaptation, I_{AHP}, is given in [13]. The approximations are also given in Appendix A.

To obtain a threshold neuron model we note that the significant role for the sodium current is for pulse generation, and assume that it does not have a strong influence on the total membrane current between spikes. Accordingly, we define a subthreshold potential $U(t)$ as the membrane potential of the neuron with blocked sodium current, i.e., according to the equation

$$C\frac{dU}{dt} = -I_{DR} - I_A - I_M - I_{\mathrm{H}} - I_L - I_{AHP} - I_a. \quad (2)$$

When the potential U crosses the threshold U^T, as defined below, a spike occurs. To take into account the duration of a spike the equations of the gating variables and the potential are not integrated during the time interval $\Delta t_{AP}=1.5$ ms after the spike initiation. Then the potential is reset to the value $U^{reset}=-40$ mV under the assumption that at this point of the repolarization phase I_{Na} is much smaller than the other membrane currents. The gating variables for the fast currents I_{DR}, I_A, and I_{H} are also reset to their fixed values, whereas the gating variables of the slow adaptation currents I_M and I_{AHP} undergo jumps from their previous values, i.e.,

$$x^{reset} = 0.26, \quad y^{reset} = 0.47 \quad \text{for } I_{DR}, \quad (3)$$

$$x^{reset} = 0.74, \quad y^{reset} = 0.69, \quad \text{for } I_A, \quad (4)$$

$$y^{reset} = 0.002, \quad \text{for } I_{\mathrm{H}}, \quad (5)$$

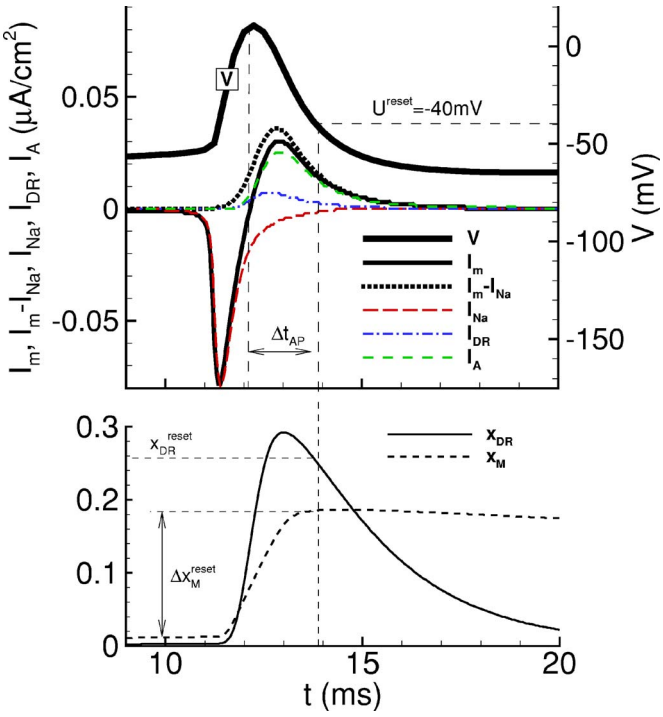

FIG. 1. (Color online) Action potential and underlying ionic currents and conductances, obtained by the complete conductance-based neuron model based on Eq. (1); here $I_m = I_{DR} + I_A + I_M + I_H + I_L + I_{AHP}$. As well, the procedure of the parameter measurement for the threshold model is illustrated, namely, measurement of the duration of the spike-descending phase, $\Delta t_{AP} = 1.5$, the reset value for the I_{DR} gating variable, x_{DR}^{reset}, and the step for the I_M gating variable, Δx_M^{reset}, at the point of crossing the level V^{reset}.

$$\Delta x^{reset} = 0.18\ (1 - x), \quad \text{for } I_M, \tag{6}$$

$$\Delta w^{reset} = 0.018\ (1 - w), \quad \text{for } I_{AHP}. \tag{7}$$

These values were calculated by the full model based on (1) in the descending phase of a spike, when $U = U^{reset}$, as shown in Fig. 1.

As a result, the potential U satisfactorily approximates the potential V of the full model on the interspike intervals, and with the threshold criteria we accurately calculate the spike times, as shown in Fig. 3 below.

We now define the firing threshold for the potential U.

B. Threshold potential U^T

The kinetics of the sodium channel depends on both the instantaneous value of the potential and its history. Here we rely on the simplest description of this dependence in terms of the functional expression of the sodium current, the action potential, by characterizing the average threshold U^T as a function of dU/dt. To calculate this dependence we use both the full neuron model (1) and its reduction (2). The dependence is obtained by applying different current steps I_a and solving Eqs. (1) and (2) for the exact, $V(t)$, and subthreshold, $U(t)$, potentials, respectively. We then define the threshold as the value of the potential U at the first spike maximum for the potential V, i.e., at $t = t_{AP}$, where t_{AP} is the time of the spike peak. The value $U^T = U|_{t=t_{AP}}$ and the corresponding $dU/dt|_{t=t_{AP}}$ give one point of the desired threshold function. We vary the input current to get a wide range of dU/dt. The resulting dependence is

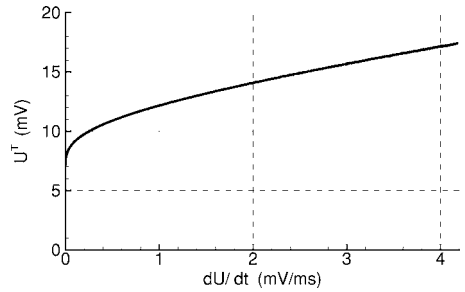

FIG. 2. Threshold potential U^T as a function of the potential slope dU/dt, comparing the solutions of Eqs. (1) and (2).

$$U^T = f(dU/dt) \tag{8}$$

shown in Fig. 2. The amplitude and the shape of the stimulating current do not explicitly take part in the dependence (8), under the assumption that the result has a low sensitivity to specific details such as the use of a current step and that only the first spike in a spike train is considered.

With this estimated dependence of spike threshold on the voltage derivative the threshold model based on Eq. (2) is completed. This model gives correct spike times for both the

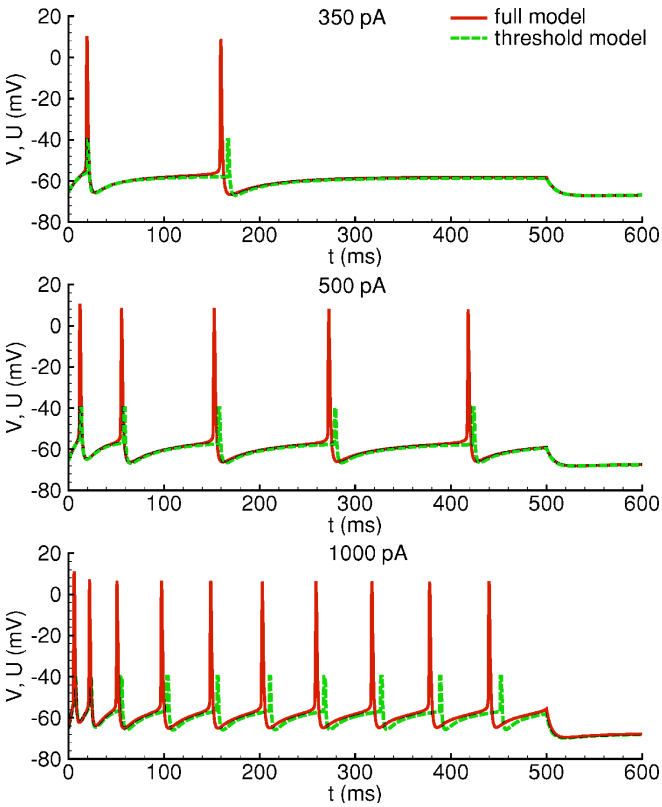

FIG. 3. (Color online) Comparison of spike trains calculated by the full conductance-based neuron model and its threshold version in the cases of stimulation by $I_a = 350$, 500, and 1000 pA.

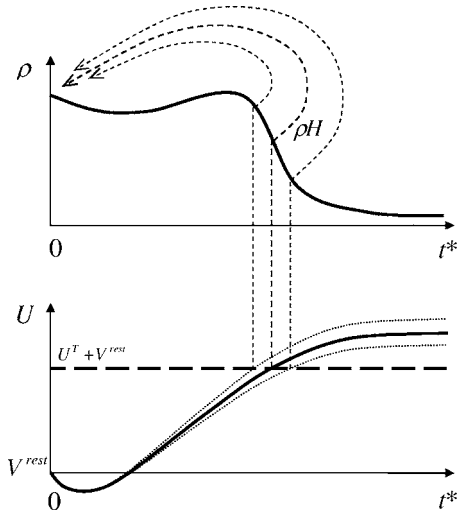

FIG. 4. Schematic representation of neuron evolution in the one-dimensional space of the time elapsed since the last spike. The density and voltage profiles are shown. Neurons move to the right till the next spike generation. After their spikes neurons transfer to the point $t^*=0$. The stationary density profile is a plateau on the interval since $t^*=0$ till about the average interspike interval, $t^* \approx 1/\rho(t,0)$, and then decays to zero.

first and subsequent spikes in a spike train in response to a constant current step, when compared to the full neuron model (Fig. 3). Since Eq. (8) considers a local parameter of the state of the neuron, the rate of change of the voltage, the threshold model maintains its precision for different stimulation amplitudes. The good agreement between threshold values for different spikes in Fig. 3 supports the choice of the particular function (8) that is used.

We now use the described single-neuron threshold model within a population density approach.

C. Population density approach

To describe the activity of a population of similar neurons receiving the sum of a common input current term and a noisy current term we consider the probability density ρ, which characterizes the number of neurons that are in a similar state of activity. Strictly speaking, ρ is the fraction of neurons per unit volume of the phase space (PS) of neuron state parameters in the mathematical limit of an infinite number of neurons. As described, in order to avoid the complexity of a high-dimensional description we reduce our consideration to a one-dimensional version of the phase space. Thus, let us introduce the one-dimensional phase space with the state variable t^*, which for any given neuron is the time elapsed since its last spike (Fig. 4). By that, we have two independent variables t and t^*, and one dependent variable $\rho=\rho(t,t^*)$. At any time t a small volume of the PS, $(t^*,t^*+\Delta t^*)$, contains a portion of neurons of the population equal to $\rho(t,t^*)\Delta t^*$. The density $\rho(t,t^*)$ is referred to as the refractory density in [4]. The value $\rho(t,0)$ represents the firing rate of the ensemble. Indeed, in accordance with [4], the population firing rate can be defined if we take a short time window Δt, count the number of spikes (summed over all neurons in the group) that occur in an interval $t,\ldots,t+\Delta t$, n_{act}, and divide by the number of neurons, N, and Δt. After taking the limits of $N\to\infty$ and $\Delta t\to 0$ [see Eq. (5.136) in [4]], the activity ν, or the rate, is $\nu(t)=\lim_{\Delta t\to 0}\lim_{N\to\infty}(1/\Delta t)n_{act}(t;t+\Delta t)/N$. In the PS of the variable t^* we have $\lim_{N\to\infty}n_{act}(t;t+\Delta t)/N=\int_0^{\Delta t}\rho(t,t^*)dt^*$, provided that Δt is smaller than the absolute refractory period. Thus, in the limit of $\Delta t\to 0$, we see that $\nu(t)\equiv\rho(t,0)$.

To describe the temporal evolution of $\rho(t,t^*)$, we note that during periods in which the neurons do not fire the value of the refractory density at (t_1,t_1^*) would be equal to that at $(t_1+\Delta t,t_1^*+\Delta t)$ as $\Delta t\to 0$, i.e., $d\rho/dt=\partial\rho/\partial t+\partial\rho/\partial t^*=0$. When neurons do fire, they instantly move to the point $t^*=0$. The rate of firing for neurons with some value of t^* is proportional to the density of neurons at that point, $\rho(t,t^*)$, and the probability for a single neuron to fire in a unit time, H. Thus, $d\rho/dt=-\rho H$. The function H is referred to in [4] as the hazard function or the spike-release probability density. Substituting the total derivative $d/dt=\partial/\partial t+\partial/\partial t^*$, we obtain that the evolution of ρ is governed by the transport equation with a source

$$\frac{\partial\rho}{\partial t}+\frac{\partial\rho}{\partial t^*}=-\rho H. \tag{9}$$

To define the spike-release probability density, H, we first consider it to be a function of both U and U^T; thus $H=H(U(t,t^*),U^T)$, i.e., the probability for a neuron to release a spike during the interval $[t,t+\Delta t]$, $H\Delta t$, depends on its subthreshold membrane potential $U=U(t,t^*)$ and on the threshold U^T. This dependence implies comparison of U with the threshold potential U^T averaged over the ensemble, which has been calculated in Sec. II B. Because the arguments of U^T are the voltage value U and its derivative dU/dt, we can treat H as a function of the function $U(t)$ only, i.e., $H=H(U(t))$.

As stated, neurons return to the point $t^*=0$ when they spike. This fact is reflected by the boundary condition for Eq. (9) which is the equation for the firing rate

$$\nu(t)\equiv\rho(t,0)=\int_{+0}^{\infty}\rho H\,dt^*. \tag{10}$$

Given the normalized ρ, the boundary condition (10) provides the conservation of the number of neurons,

$$\int_0^{\infty}\rho\,dt^*=1.$$

As mentioned above, the value $\rho(t,0)$ is the firing rate of the ensemble. In a stationary or quasistationary regime, $\rho(t,0)$ corresponds to the firing rate of a single neuron with a mean threshold U^T.

To define the membrane potential U for all t^*, we rewrite Eq. (2) by substituting the total derivative $d/dt=\partial/\partial t+\partial/\partial t^*$:

$$C\left(\frac{\partial U}{\partial t}+\frac{\partial U}{\partial t^*}\right)=-I_{DR}-I_A-I_M-I_H-I_L-I_{AHP}-I_a. \tag{11}$$

Similarly, we get the equations for the gating variables of all the active ionic currents, i.e.,

$$\frac{\partial x}{\partial t}+\frac{\partial x}{\partial t^*}=\frac{x_\infty(U)-x}{\tau_x(U)},\quad \frac{\partial y}{\partial t}+\frac{\partial y}{\partial t^*}=\frac{y_\infty(U)-y}{\tau_y(U)} \tag{12}$$

with $x_\infty(U)$, $\tau_x(U)$, $y_\infty(U)$, $\tau_y(U)$ taken from [12].

According to the threshold model described above, the voltage and the gating variables of the ionic currents are not integrated within the interval $0<t^*<\Delta t_{AP}$, i.e., the boundary conditions for Eqs. (11) and (12) are $U(t,\Delta t_{AP})=U^{reset}$; $x(t,\Delta t_{AP})=x^{reset}$, $y(t,\Delta t_{AP})=y^{reset}$, where x^{reset} and y^{reset} are taken from Eqs. (3)–(5). The reset values for the adaptation current are calculated, incrementing the values at the peak of spike-release distribution in the t^* space:

$$\Delta x^{reset}=0.18[1-x(t,t^{*p})],\quad \text{for } I_M, \tag{13}$$

$$\Delta w^{reset}=0.018[1-w(t,t^{*p})],\quad \text{for } I_{AHP}, \tag{14}$$

where t^{*p} is such that $\rho(t,t^{*p})H(t,t^{*p})=\max_{0<t^*<+\infty}\rho(t,t^*)H(t,t^*)$.

We now define the function H, given the membrane potential U and its time derivative.

D. The spike-release probability density H

A formula to calculate the spike-release probability density H should consider a model of noise and the variation of the cellular parameters and of the synaptic inputs over the entire neuron population. Here we assume that the functional impact of these factors may be expressed in an additive Gaussian noise term affecting the potential of a given neuron. The other parameters governing the neuron are given by their average over all the neurons at t^*. The expected firing rate for this neuron is given by the spike-release probability density for a population.

For the undisturbed subthreshold potential $U(t)$ we write down again Eq. (2),

$$C\frac{dU}{dt}=-I_{tot}(U,t), \tag{15}$$

where $I_{tot}=I_{DR}+I_A+I_M+I_H+I_L+I_{AHP}+I_a$ is the total current.

For the disturbed subthreshold potential $V'(t)$ we write the equation

$$C\frac{dV'}{dt}=-I_{tot}(V',t)+\sigma g_{tot}^0\xi(t), \tag{16}$$

where $\xi(t)$ is the Gaussian white noise characterized by its mean value $\langle\xi(t)\rangle=0$, and autocorrelation $\langle\xi(t)\xi(t')\rangle=\tau_m^0\delta(t-t')$; $g_{tot}(V',t)=g_{DR}+g_A+g_M+g_H+g_L+g_{AHP}$ is the total conductance, g_{tot}^0 is the total conductance at the rest steady state, and $\tau_m^0=C/g_{tot}^0$ is the membrane time constant at the rest steady state. The neuron fires when the potential V' crosses the threshold U^T. From the comparison of Eq. (2) with Eq. (16) we can conclude that at least for stable solutions if the noise amplitude σ tends to 0 the expected value of $V'(t)$ is equal to $U(t)$. Analogously, it holds for small noise that $g_{tot}(V',t)\approx g_{tot}(U,t)$. In general, the expected values of the channel conductances depend not only on the mean voltage but on the voltage fluctuations as well. However, actually, this effect is not significant. Rather, the greatest effect is on the adaptation currents, when relatively fast positive voltage fluctuations tend to increase the adaptation conductances, which slowly decay afterward. Here we neglect these effects and estimate the total conductance by its value in the zero-noise case. Thus, we can linearize the current $I_{tot}(V',t)\approx I_{tot}(U,t)+g_{tot}(U,t)(V'-U)$. After subtraction of Eq. (15) from Eq. (16) we obtain the equation for the voltage fluctuations

$$C\frac{d(V'-U)}{dt}=-g_{tot}(U,t)(V'-U)+\sigma g_{tot}^0\xi(t). \tag{17}$$

We then neglect the dynamics of $g_{tot}(U,t)$, i.e., $dg_{tot}/dt\approx 0$, $d\tau_m/dt\approx 0$, under the assumption that just prior to crossing the threshold the voltage evolution depends only on the value of $g_{tot}(U,t)$ and not on its temporal derivative. Dividing Eq. (17) by $g_{tot}^0(U,t)\sigma$ and introducing the variable for the voltage fluctuations scaled by the noise amplitude, $u\equiv g_{tot}(U,t)\times(V'-U)/g_{tot}^0\sigma$, we obtain the equation

$$\tau_m(U,t)\frac{du}{dt}=-u+\xi(t), \tag{18}$$

where $\tau_m(U,t)=C/g_{tot}(U,t)$ is the membrane constant. The value $\sigma/\sqrt{2}$ corresponds to the membrane potential dispersion in the steady state, i.e., $\sigma_V=\sigma/\sqrt{2}$. The neuron fires at the threshold $T(t)\equiv g_{tot}(U,t)[U^T-U(t)]/g_{tot}^0\sigma$.

We can find the expected firing rate for the neuron by considering the corresponding Fokker-Planck equation for the probability density of a neuron to be in the state u, $\tilde{\rho}(t,u)$, which is

$$\tau_m(U,t)\frac{\partial\tilde{\rho}}{\partial t}+\frac{\partial}{\partial u}\left(u\tilde{\rho}-\frac{1}{2}\frac{\partial\tilde{\rho}}{\partial u}\right)=0 \tag{19}$$

with the boundary conditions $\tilde{\rho}(t,-\infty)=\tilde{\rho}(t,T(t))=0$ and the initial Gaussian distribution. The expected firing rate is given by the flux term written in large parentheses calculated at the threshold $u=T(t)$ and divided by τ_m. It is thus defined as

$$H(U(t))=-\frac{1}{2\tau_m}\left.\frac{\partial\tilde{\rho}}{\partial u}\right|_{u=T(t)}. \tag{20}$$

A good approximation for the function $H(U(t))$ can be found by considering two particular cases, the self-similar solution A for the case of a slow change in the voltage U, and the frozen Gaussian solution B for the case of fast-increasing voltage U. The self-similar solution means that the probability density distribution changes in amplitude but not in shape. The stationary equation for the shape of $\tilde{\rho}(t,u)$ is an ordinary differential equation and can be solved analytically. The frozen Gaussian solution is valid when the difference between the mean and threshold potentials changes faster than the probability density distribution reshapes due to diffusive influence of noise. The considered particular cases are limit cases in the sense that B is zero in the unvarying $U(t)$ regime, and A is negligible in the fast-varying $U(t)$ regime. By their physical meanings, the activity B occurs due to the

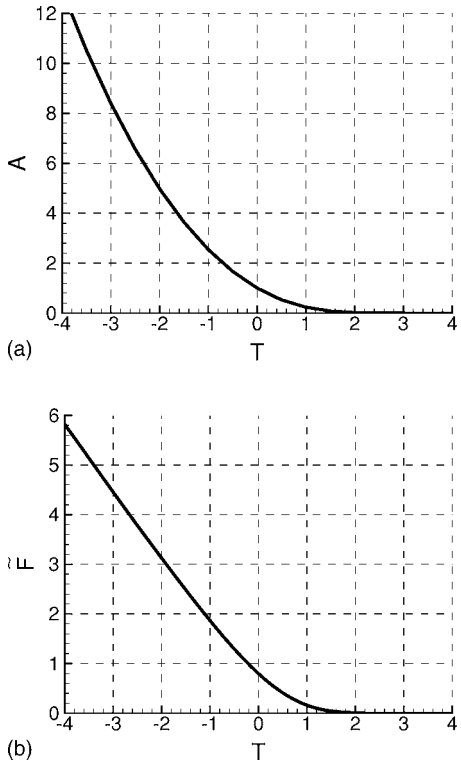

FIG. 5. Components of approximate hazard function. (a) Function A characterizes the firing probability of a neuron at given dimensionless distance to threshold T in the regime of slow changes of T. (b) Dimensionless function $\tilde{F}(T)$, defined by Eq. (21), characterizes the firing probability in the regime of fast changes of T.

"movement" of the threshold boundary $u=T(t)$ toward the probability density function (PDF), whereas the activity A occurs due to "flow" through a threshold boundary $u=T$ because of transfer and diffusion processes changing the PDF. These processes providing "sources" of neuron leakage are independent. Relying on this fact, we suppose and find to be true that the activities are additive, i.e., the sum of the solutions $A+B$ gives a satisfactory approximation for H in any arbitrary case of neuron stimulation. The result is the following formula:

$$H(U(t)) = \frac{1}{\tau_m}[A(T(U)) + B(U,dU/dt)], \tag{21}$$

where $A(T)$ is given by the curve in Fig. 5(a) and

$$B(U,dU/dt) = -\sqrt{2}\tau_m\left[\frac{dT}{dt}\right]_+ \tilde{F}(T), \quad \tilde{F}(T) = \sqrt{\frac{2}{\pi}}\frac{\exp(-T^2)}{1+\mathrm{erf}(T)}. \tag{22}$$

The function $\tilde{F}(T)$ is shown in Fig. 5(b); $[x]_+=x$ for $x>0$ and zero otherwise.

Thus, we have obtained the system of equations (9)–(12), (3)–(5), (13), (14), (21), and (22) governing the activity of a neuronal ensemble. The numerical method to solve this system is described in Appendix C

III. RESULTS

For justification of the proposed method we compare it to simulations of a discrete set of individual neurons given a step stimulation, thus illustrating the quality of the transient regime approximation. Furthermore, we analytically derive the rate-current curve from the proposed population model and compare with the known analytical result in the case of integrate-and-fire neurons. Finally, as a demonstration of how to apply the model to an interconnected population and as an independent result consistent with experiment, we present simulations of interictal-like bursts.

A. Population and individual neuron simulations

In this section, we present simulations for a population of uncoupled neurons, all of which receive common input from an external source and noise with the dispersion $\sigma=0.2\sqrt{2}U^T$ to get $\sigma_V \approx 0.2U^T$, where this value estimates typical voltage fluctuations or dispersion of voltage thresholds. Thus in the Eq. (1) we consider an extra term $\sigma g_{tot}^0 \xi(t)$, where $\xi(t)$ is the Gaussian white noise characterized by its mean value $\langle \xi(t)\rangle=0$ and autocorrelation $\langle \xi(t)\xi(t')\rangle=\tau_m^0\delta(t-t')$. We compare the population density approach with direct individual neuron simulations. The population density equations with the same dispersion σ were solved numerically.

As a response to a rapid change in input, the firing rate transiently jumps up before returning to a new steady-state response as seen in Figs. 6(a)–6(e). The distributions of the potential U and the density ρ in the PS at one instant in time are shown in Fig. 6(f). The steep gradient of the density corresponds to near-threshold potentials. Shown in Figs. 6(a)–6(c) are the simulations without adaptation currents I_M and I_{AHP} for I_a=200, 300, and 500 pA, correspondingly. Taking into account only I_M, or both I_M and I_{AHP}, changes the rate as shown in Figs. 6(d) and 6(f), respectively. With adaptation, the population model slightly exaggerates this dissipation effect. On the whole, the rate obtained by the population model well approximates the rate of a set of individual neurons for different stimulus strengths. As a comparison, we also plot the rate obtained by the firing-rate model in Fig. 6(b) (dashed line), calculated by the steady-state rate-voltage dependence $\nu=\nu^{SS}(U(t,\infty))$.

The responses to oscillating input current are shown in Fig. 7 for the cases of taking into account only I_M adaptation current [Fig. 7(a)] or both I_M and I_{AHP} adaptation currents [Fig. 7(b)]. The adaptation currents, oscillating input, and noise result in high variability of the individual neuron voltage traces [examples are shown in Fig. 7(b)] and, consequently, different amplitudes of population rate peaks. The population model firing rate compares well with the averaged firing rate of individual neurons.

B. Predictions: A model of interictal-like bursts

The proposed formulation may also be applied for synaptically connected networks. To demonstrate this point we simulate the activity of a recurrent pyramidal cell network including all-to-all connectivity by excitatory synapses. Syn-

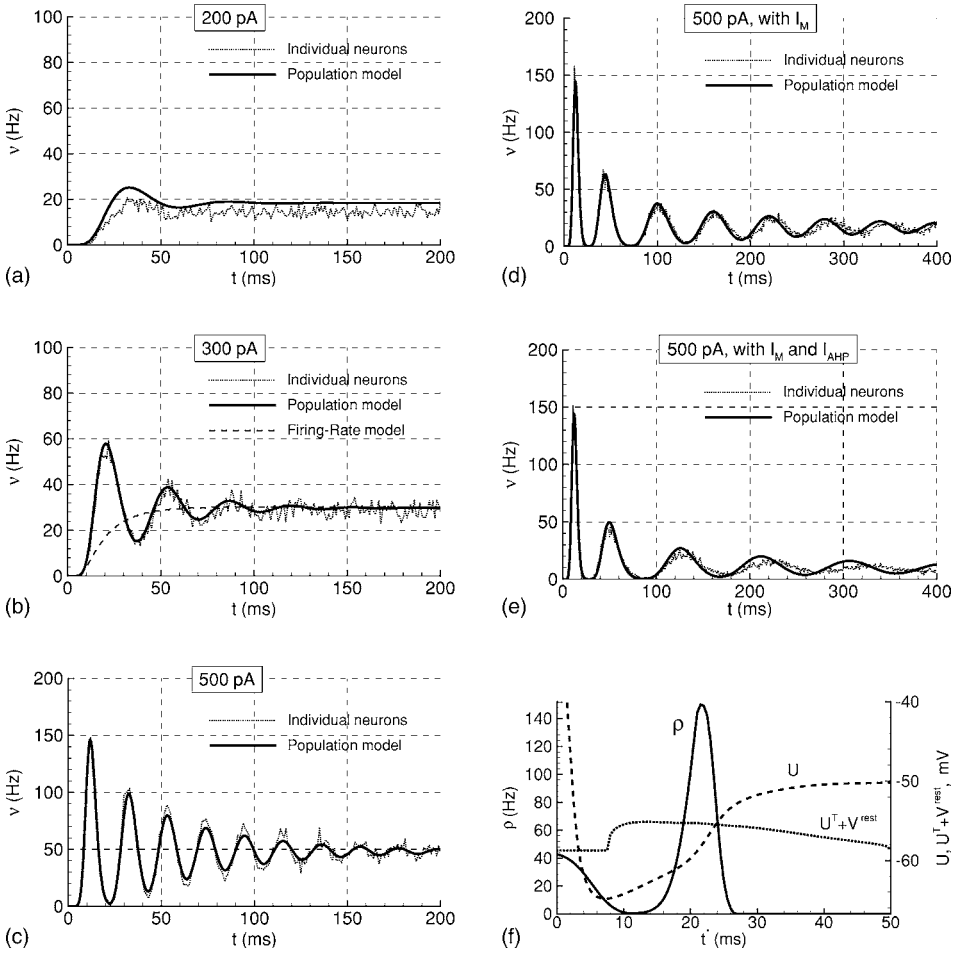

FIG. 6. Transient response of the population firing rate to a rapid change in input. Beginning at $t=0$, the excitatory input current to the uncoupled nonadapting neurons of a single population is stepped up to 200, 300, and 500 pA, respectively, in (a), (b), and (c). Similar simulations which take into account the slow adaptation current I_M alone, and both I_M and I_{AHP}, are shown in (d) and (e). The firing rate transiently jumps up before returning to a new steady-state response. The population model firing rate (solid line) compared with the averaged firing rate of individual neurons. (f) Distributions of the potential $U(t_1,t^*)$, the density $\rho(t_1,t^*)$, and the threshold potential U^T changing with dU/dt across the time elapsed since the last spike, t^*, corresponding to (e) at the time $t_1=35$ ms. For comparison, the rate obtained by the firing-rate model is shown in (b) (dashed line), calculated by the steady-state rate-voltage dependence $\nu = \nu^{SS}(U(t,\infty))$.

aptic noise is approximated by an additive white noise term, as described in Sec. III A. In this case the input current consists of two terms, $I_a(t)=I_{ext}(t)+I_S(t)$. The first term I_{ext} is the applied external current, taken to be 150 pA and starting at $t=0$. The second term $I_S(t)$ is the synaptic current governed by the population firing rate, i.e.,

$$I_S(t) = g_S(t)[U(t) - V_S], \tag{23}$$

$$\tau_S^2 \frac{d^2 g_S(t)}{dt^2} + 2\tau_S \frac{dg_S(t)}{dt} + g_S(t) = \bar{g}_S \tau \nu(t - \tau_d), \tag{24}$$

where $\nu(t)$ is the presynaptic population firing rate. As noted previously for the population model $\nu(t)=\rho(t,0)$, whereas for the direct simulation $\nu(t)$ is given by the spike rate, normalized over the total number of neurons. The remaining terms are equivalent for the two models: τ_S is the synaptic time constant, τ_d is the synaptic delay, $\bar{g}_S$ is the maximum synaptic conductance, V_S is the synaptic current reversal potential, and τ is the scaling time constant fixed to be equal to 1 ms. For purposes of illustration the following values were used: $\tau_S=5.4$ ms, $\tau_d=1$ ms, $V_S=5$ mV, $\bar{g}_S=1$ mS/cm^2. As shown in Fig. 8 the population model shows quite similar behavior to simulations of a recurrent network made of explicit individual neurons. In the considered situation the neural network is very sensitive to any changes of its parameters, because a weak disturbance of the network might provoke an excitation of a small fraction of neurons which evoke a cascade activation of the total population. When this instability is taken into account the simulations by the two models may be considered quite similar, with an error in the interburst interval of only 14%. As mentioned in Sec. II D the main source of the solution deviation is that in contrast to the supposition made the total conductance is governed not only by the mean potential but by the potential fluctuations as well. Mainly, the adaptation ionic current conductances are underestimated. Thus a correction could be made, introducing an increment to the maximum conductance of AHP current, $\bar{g}_{AHP}$, depending on σ_V.

Taking into account that the choosen values of τ_S and V_S correspond to the characteristics of somatically measured aminomethylphosphonic acid (AMPA)-receptor-mediated current [14], we propose that this population activity relates to the physiological interictal activity, given that one suggested mechanism involves a population of pyramidal cells recurrently connected by AMPA-receptor-mediated synapses. The shape of the bursts is similar to one observed in the disinhibited cornus ammonis sector 1 (CA1) minislices [15]. Under these conditions an important prediction of the model is that the key mechanism for shaping the bursts are the adaptation currents.

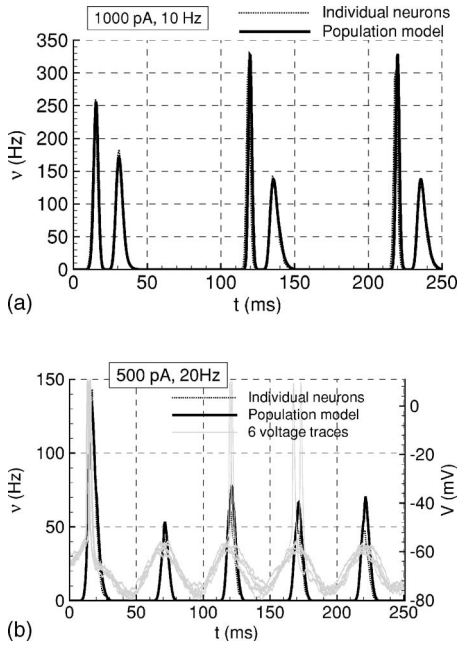

FIG. 7. Responses to oscillating input current. The population model firing rate (solid line) compares well with the averaged firing rate of individual neurons (dotted line). (a) Only I_M adaptation current was taken into account; the parameters of the input were 1000 pA, 10 Hz. (b) Both I_M and I_{AHP} adaptation currents, 20 Hz oscillating input current of 500 pA amplitude, and noise result in high variability of the individual neuron voltage traces (examples are shown in gray lines) and, consequently, different amplitudes of population rate peaks.

C. Verification by an analytical solution: Steady-state firing of integrate-and-fire neurons

For the verification of the proposed approach based on the assumptions made for the derivation of the hazard function, we compare the steady-state population firing rate calculated by the proposed RDA to the known analytical solution [16] obtained for linear integrate-and-fire neurons with constant thresholds, receiving, as above, an injected current I_a and an additive white Gaussian noise with the dispersion σ. Here we also set the reset potential equal to V_L.

The solution from [16] is as follows:

$$\nu = \left(\tau_m \sqrt{(\pi)} \int_{(V_L - x)/\sigma}^{(U^T - x)/\sigma} \exp(u^2)[1 + \mathrm{erf}(u)]du \right)^{-1} \quad (25)$$

where $\tau_m = C/g_L$ and $x = V_L + I_a/g_L$ is the asymptotic potential.

In this particular case the equations of the RDA can be written as follows:

$$\frac{du}{dt'} = -u + a,$$

$$\frac{d\rho}{dt'} = -\rho A(T) + \rho \frac{dT}{dt'} \sqrt{2} \tilde{F}(-T),$$

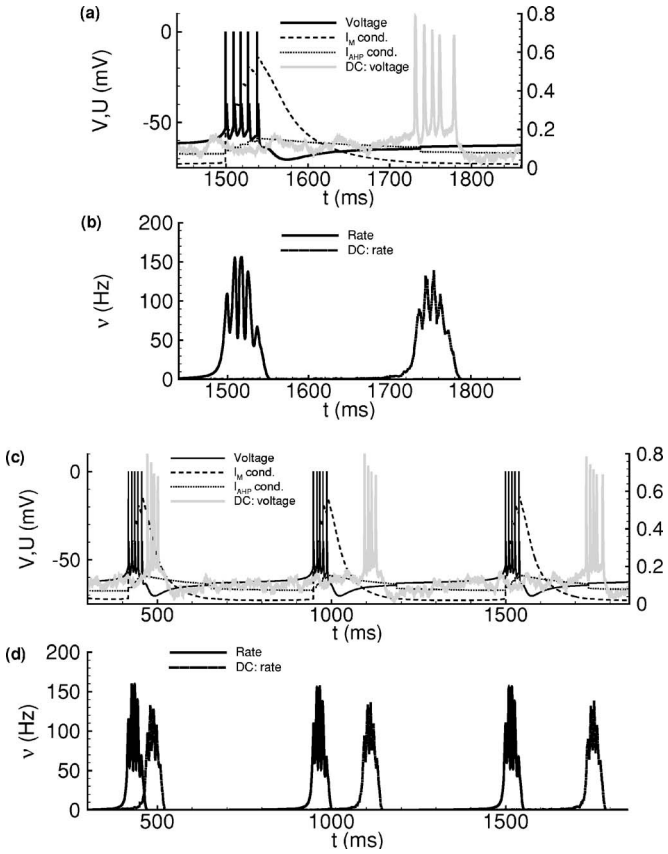

FIG. 8. Repeating bursts in the population of interconnected pyramidal cells, obtained by direct simulation (DS) of a great number (4000) of all-to-all interconnected neurons and by the population model. The two parameters, the constant external current $I_{ext} = 150$ pA and the maximum synaptic conductance $\bar{g}_S = 1$ mS/cm^2, were arbitrarily chosen. The synaptic conductance time constant $\tau_S = 5.4$ ms corresponds to known kinetics of AMPA-receptor synaptic conductance [14]. Shown in two time scales are (a),(c) spike trains for the representative neuron in the population model (solid line) and in DS (gray line), as well as the dimensionless conductances of adaptation currents I_M and I_{AHP} (dashed and dotted lines, respectively); (b),(d) firing rate in the population model (solid line) and in DS (dotted line). The effect of the adaptation currents provides interburst pauses, whereas refractory and excitation properties provide complex five-peak shapes of the population spikes.

$$\int_0^\infty \rho \, dt' = 1, \quad u(0) = 0,$$

$$\nu \equiv \rho(0),$$

with $u = (U - V_L)/(U^T - V_L)$, $t' = t^*/\tau_m$, $T = (U^T - U)/\sigma$, $a = I_a/g_L(U^T - V_L)$. The solution by the RDA for $\nu(I_a)$ is expressed by

$$\nu = \left[\tau_m \int_0^a \exp\left(- \int_0^{u'} \frac{\tilde{H}(u)}{a - u} du \right) \Big/ (a - u')du' \right]^{-1},$$

$$\tilde{H}(u) = A(T) + (a - u)(U^T - V_L)/\sigma\sqrt{2}\tilde{F}(-T). \quad (26)$$

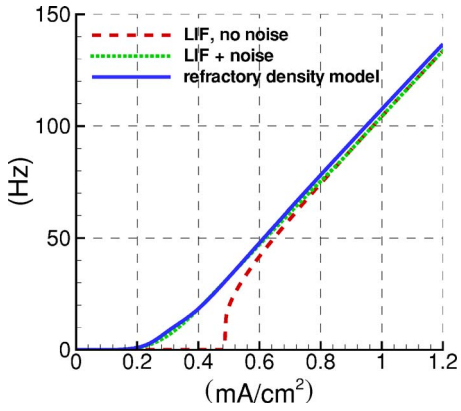

FIG. 9. (Color online) Steady-state firing of a linear leak integrate-and-fire neuron with and without noise. The proposed RDA model (blue solid curve) in this particular case quite well reproduces the green dotted curve—the analytical solution known for this case [16].

The results of comparison of the formulas (25) with (26) are shown in Fig. 9. Good agreement of the solutions justifies that the derived formulas for the hazard-function works well in the arbitrary regimes of neural stimulation.

IV. DISCUSSION

We have generalized the known refractory density approach for the case of realistic, adaptive, neurons. The obtained system of equations is intended to approximate an infinite set of similar pyramidal neurons receiving a common input and dispersed by noise, including the case of a synaptically connected network. Here we outline the advantages of the model and its possible extensions.

Previous population density approaches for studying the dynamics of neuronal populations have considered distributions of neurons across either the membrane voltage or the time passed since the last spike. The former method has been based on the integrate-and-fire neuron [11,4,17,3,18]. The latter method, that is the refractory density approach, is based on the spike response model (SRM) [2,4,19]. As a more general single-neuron model than the integrate-and-fire neuron, the SRM can more precisely describe the neuron dynamics. Moreover, in contrast to the membrane potential, the time since the last spike monotonically changes with time (modulo spike times) and better describes the state of a neuron, in particular, its refractory properties. However, the SRM considers only input current [4,19], while in general neuronal input is composed of a current term and a conductance term [20]. Thus, the SRM approach neglects shunting effect of the input. Also, a generalization of the SRM on the case of adaptive neuron is not known to the authors.

The refractory density approach proposed in the present paper is based on a single-neuron model which is different from the SRM. The SRM supposes that the membrane potential is the sum of a term reflecting the evoked spike and a postsynaptic term reflecting the synaptic input. In contrast, the present paper states that instead of the decomposition it is sufficient to omit the sodium current when calculating the potential relative to the spike threshold. As a consequence, the approach has several advantages in comparison to the SRM-based RDA and other known one-dimensional population models. First, the threshold calculated as a one-parametric dependence on the potential slope provides better accuracy because it implicitly reflects the activity of the omitted sodium channels. Second, using the current approach it is possible to take into account additional fast ionic currents as well as slow currents, due to the explicit conductance-based formulation of the approach. Third, the current model is described by partial differential equations, which are easier to solve than integral-differential equations such as used in [4,11]. Finally, due to the obtained analytical solutions of the Fokker-Planck equation in the particular cases of weak and strong stimulation, the proposed approximation for the spike-release probability density function H, or hazard function, is quite precise and does not contain free parameters. As a result, the full system of equations of the population model does not contain free parameters, when derived from a full single-neuron model and assuming a fixed noise amplitude.

The computational efficiency of the population modeling in the framework of the density equation is significantly better than that of the direct simulation of explicit individual neurons. In particular, for the proposed model this follows as it belongs to the class of one-dimensional density equation approaches, for which estimations of computation efficiency can be found in [11,4]. These results, which are consistent with our observations for the simulations presented here, demonstrate that the population density approach is between 10 and 100 times faster than the individual neuron simulations. For instance, our simulation of 4000 individual neurons, shown in Fig. 6(e), lasted 20 min and still holds fluctuations in the firing-rate curve, whereas the similar simulation by the population model on the finest grid lasted about 1 min.

In the present paper we have shown how the approach may be used to reproduce known network behavior, such as inter-ictal spikes. We suggest that when the proposed model is linked with a similar model for interneuron population [5], one can simulate additional network dynamics, for example gamma oscillations. Furthermore, by taking into account the topology of spatial connections, the model should reproduce inhomogeneous network phenomena, such as the propagation of activity along the cortical slice, and postsynaptic potentials evoked by extracellular stimulation. Future work could also generalize the presented model to consider conductance noise when the neurons interact synaptically.

Thus, the proposed model of a single population of neurons can be used as a core of a population model of cortical tissue that can be quantitatively fitted to intracellular experimental recordings. The reduced evaluation time of the proposed refractory density approach should facilitate modeling more complex neural networks, as compared to the evaluation of networks based on explicit individual neuron models. The refractory density approach may be an important tool for the implementation of truly large-scale models of the networks in the brain.

ACKNOWLEDGMENTS

The authors thank Nicolas Brunel for comments on the manuscript. The work was supported by an HFSP Research Grant No. RGP0049 and a Russian Foundation of Basic Research Grant No. 04-01-00048a.

APPENDIX A: THE INTRINSIC CURRENTS

The single-compartment pyramidal neuron was described by the conventional equation (1). Different types of ionic currents were inserted, including the leak current I_L, the fast sodium current I_{Na}, the voltage-dependent potassium currents responsible for spike repolarization, I_{DR} and I_A, the voltage-dependent potassium current that contributes to spike frequency adaptation, I_M, the voltage-dependent cation current I_{H}, and the calcium-dependent potassium current that also contributes to spike frequency adaptation, I_{AHP}. The approximating formulas for the currents I_{Na}, I_{DR}, I_A, I_M, and I_{H} were adapted from [12]; the approximation for I_{AHP} was taken from [13].

The sodium current I_{Na} is given by

$$I_{\mathrm{Na}}(t) = \bar{g}_{\mathrm{Na}} x_1(t)[V(t) - V_{\mathrm{Na}}], \tag{A1}$$

$$x_1 + x_2 + x_3 + x_4 = 1, \tag{A2}$$

$$\frac{dx_i}{dt} = \sum_{j=0,\ j\neq i}^{4} A_{j,i}x_j - x_i \sum_{j=0,\ j\neq i}^{4} A_{i,j}, \quad i = 1,2,3, \tag{A3}$$

$$A_{1,2} = 3\ \mathrm{ms}^{-1}, \quad A_{1,3} = f_1^{1,3}(V), \quad A_{1,4} = f_1^{1,4}(V),$$

$$A_{2,1} = 0, \quad A_{2,3} = f_2^{2,3}(V), \quad A_{2,4} = 0,$$

$$A_{3,1} = f_1^{3,1}(V), \quad A_{3,2} = 0, \quad A_{3,4} = f_2^{3,4}(V),$$

$$A_{4,1} = f_1^{4,1}(V), \quad A_{4,2} = 0, \quad A_{4,3} = 0,$$

$$f_1^{i,j}(V) = \left\{ \tau_{min}^{i,j} + 1/\exp\left(\frac{V - V_{1/2}^{i,j}}{k^{i,j}} \right) \right\}^{-1},$$

$$f_2^{i,j}(V) = \left\{ \tau_{min}^{i,j} + \left[(\tau_{max}^{i,j} - \tau_{min}^{i,j})^{-1} + \exp\left(\frac{V - V_{1/2}^{i,j}}{k^{i,j}} \right) \right]^{-1} \right\}^{-1}.$$

Note that there is an implicit coefficient of the exponential term of 1/ms in the equations for $f_1^{i,j}(V)$ and $f_2^{i,j}(V)$. Also

$$\tau_{min}^{1,3} = 1/3\ \mathrm{ms}, \quad V_{1/2}^{1,3} = -51\ \mathrm{mV}, \quad k^{1,3} = -2\ \mathrm{mV},$$

$$\tau_{min}^{1,4} = 1/3\ \mathrm{ms}, \quad V_{1/2}^{1,4} = -57\ \mathrm{mV}, \quad k^{1,4} = -2\ \mathrm{mV},$$

$$\tau_{min}^{2,3} = 1\ \mathrm{ms}, \quad V_{1/2}^{2,3} = -53\ \mathrm{mV}, \quad k^{2,3} = -1\ \mathrm{mV},$$

$$\tau_{max}^{2,3} = 100\ \mathrm{ms},$$

$$\tau_{min}^{3,1} = 1/3\ \mathrm{ms}, \quad V_{1/2}^{3,1} = -42\ \mathrm{mV}, \quad k^{3,1} = 1\ \mathrm{mV},$$

$$\tau_{min}^{3,4} = 1\ \mathrm{ms}, \quad V_{1/2}^{3,4} = -60\ \mathrm{mV}, \quad k^{3,4} = -1\ \mathrm{mV},$$

$$\tau_{max}^{3,4} = 100\ \mathrm{ms},$$

$$\tau_{min}^{4,1} = 1/3\ \mathrm{ms}, \quad V_{1/2}^{4,1} = -51\ \mathrm{mV}, \quad k^{4,1} = 1\ \mathrm{mV}.$$

The voltage-dependent potassium current I_{DR} is given by

$$I_{DR}(t) = \bar{g}_{DR} x(t) y(t)[V(t) - V_{DR}], \tag{A4}$$

$$\frac{dx}{dt} = \frac{x_\infty(V) - x}{\tau_x(V)}, \quad \frac{dy}{dt} = \frac{y_\infty(V) - y}{\tau_y(V)},$$

$$\tau_x = 1/(a+b) + 0.8\ \mathrm{ms}, \quad x_\infty = a/(a+b),$$

$$a = 0.17 \exp[(V+5) \times 0.090]\ \mathrm{ms}^{-1},$$

$$b = 0.17 \exp[-(V+5) \times 0.022]\ \mathrm{ms}^{-1},$$

$$\tau_y = 300\ \mathrm{ms}, \quad y_\infty = 1/\{1 + \exp[(V+68) \times 0.038]\}.$$

The voltage-dependent potassium current I_A is given by

$$I_A(t) = \bar{g}_A x^4(t) y^3(t)[V(t) - V_A], \tag{A5}$$

$$\frac{dx}{dt} = \frac{x_\infty(V) - x}{\tau_x(V)}, \quad \frac{dy}{dt} = \frac{y_\infty(V) - y}{\tau_y(V)},$$

$$\tau_x = 1/(a_x + b_x) + 1\ \mathrm{ms}, \quad x_\infty = a_x/(a_x + b_x),$$

$$a_x = 0.08 \exp[(V+41) \times 0.089]\ \mathrm{ms}^{-1},$$

$$b_x = 0.08 \exp[-(V+41) \times 0.016]\ \mathrm{ms}^{-1},$$

$$\tau_y = 1/(a_y + b_y) + 2\ \mathrm{ms}, \quad y_\infty = a_y/(a_y + b_y),$$

$$a_y = 0.04 \exp[-(V+49) \times 0.11]\ \mathrm{ms}^{-1},$$

$$b_y = 0.04\ \mathrm{ms}^{-1}.$$

The voltage-dependent potassium current I_M is given by

$$I_M(t) = \bar{g}_M x^2(t)[V(t) - V_M], \tag{A6}$$

$$\frac{dx}{dt} = \frac{x_\infty(V) - x}{\tau_x(V)},$$

$$\tau_x = 1/(a+b) + 8\ \mathrm{ms}, \quad x_\infty = a/(a+b),$$

$$a = 0.003 \exp[(V+45) \times 0.135]\ \mathrm{ms}^{-1},$$

$$b = 0.003 \exp[-(V+45) \times 0.090]\ \mathrm{ms}^{-1}.$$

The cation current I_{H} is given by

$$I_{\mathrm{H}}(t) = \bar{g}_{\mathrm{H}} y(t)[V(t) - V_H], \tag{A7}$$

$$\frac{dy}{dt} = \frac{y_\infty(V) - y}{\tau_y},$$

$$\tau_y = 180 \text{ ms}, \quad y_\infty = 1/\{1 + \exp[(V+98) \times 0.075]\} \text{ ms}^{-1}.$$

The adaptation current I_{AHP} is given by

$$I_{AHP}(t) = \bar{g}_{AHP} w(t)[V(t) - V_{AHP}], \tag{A8}$$

$$\frac{dw}{dt} = \frac{w_\infty(V) - w}{\tau_w(V)},$$

$$\tau_w = 400 \times 5/\{3.3 \exp[(V+35)/20] + \exp[-(V+35)/20]\} \text{ ms},$$

$$w_\infty = 1/\{1 + \exp[-(V+35)/10]\};$$

where the reversal potentials and maximum conductances are

$$V_{DR} = -70 \text{ mV}, \quad V_A = -70 \text{ mV}, \quad V_M = -80 \text{ mV},$$

$$V_H = -17 \text{ mV}, \quad V_{AHP} = -70 \text{ mV},$$

$$\bar{g}_{\text{Na}} = 1.2 \ \mu\text{S}, \quad \bar{g}_{DR} = 0.4 \ \mu\text{S}, \quad \bar{g}_A = 2.3 \ \mu\text{S},$$

$$\bar{g}_M = 0.4 \ \mu\text{S}, \quad \bar{g}_H = 0.003 \ \mu\text{S}, \quad \bar{g}_{AHP} = 0.32 \ \mu\text{S},$$

$$\bar{g}_L = 0.025 \ \mu\text{S} \quad (\text{i.e., } \tau_m = 14.4 \text{ ms}),$$

$$V_L = -61.22 \text{ mV} \quad (\text{i.e., } V_{rest} = -65.7 \text{ mV}).$$

APPENDIX B: APPROXIMATION OF THE HAZARD FUNCTION FOR THE REFRACTORY DENSITY EQUATION OF A NEURAL POPULATION MODEL

The problem to be solved is to find the proper approximation for the spike release probability density function H, or the hazard function. To this end, we build a linearized model of voltage fluctuations near a time-varying mean value of $U(t)$ due to noise. The equation describes the voltage evolution until its first passage of the threshold U^T. As we do not follow the neuron after its first spike-time moment, we refer to this as the first-passage problem. Then, we write the corresponding Fokker-Planck equation for the first-passage problem, find its self-similar solution for the case of the so-called subthreshold regime of stimulation [4], or, more precisely, for a slow-varying $U(t)$, and furthermore describe the known stationary, "frozen" Gaussian solution for the case of superthreshold regime, that is, a fast-varying $U(t)$. Since the neuron activity in the first-passage problem coincides with the hazard function, the solutions in these two particular cases give two simple dependences of the hazard function H on the voltage $U(t)$, denoted as A for the slow-varying $U(t)$ regime and B for the fast-varying $U(t)$ regime. The particular cases that we consider are limit cases in the sense that B is zero in the unvarying $U(t)$ regime, and A is negligible in the fast-varying $U(t)$ regime. By their physical meanings, the activity B occurs due to the movement of the threshold boundary towards the probability density function, whereas the activity A occurs due to flow of the PDF through a threshold boundary due to transfer and diffusion processes changing the PDF. We then suppose and find to be true that the sum of the solutions $A+B$ gives a satisfactory approximation for H for arbitrary stimulation regimes. This result is verified by comparison with the numerical solution of the Fokker-Planck equation.

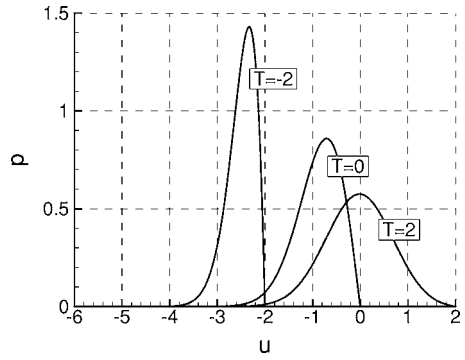

FIG. 10. Shapes p of self-similar distributions for three given values of $T=-2,0,2$ according to Eq. (B6).

Let us consider the linearized single-neuron model for the nondimensional voltage fluctuations, $u(t)$, about the mean voltage $U(t)$ with the membrane time constant $\tau_m(t)$, given a white noise amplitude σ. The model is described by Eq. (18). The nondimensional voltage crosses the threshold when $u = T(t)$ The corresponding Fokker-Planck equation for the probability density distribution $\tilde{\rho}(t,u)$ is as follows:

$$\tau_m \frac{\partial \tilde{\rho}}{\partial t} + \frac{\partial}{\partial u}\left(-u\tilde{\rho} - \frac{1}{2}\frac{\partial \tilde{\rho}}{\partial u}\right) = 0 \tag{B1}$$

with the boundary conditions $\tilde{\rho}(t,T(t))=0$, $\tilde{\rho}(t,-\infty)=0$, and the initial condition

$$\tilde{\rho}(0,u) = 1/\sqrt{\pi}\exp(-u^2). \tag{B2}$$

We can explicitly describe the shape $p(t,u)$ and the amplitude $\rho(t)$ of the probability distribution $\tilde{\rho}(t,u)$ by the substitution

$$\tilde{\rho}(t,u) = \rho(t)p(t,u) \tag{B3}$$

such that

$$\rho(t) = \int_{-\infty}^{T(t)} \tilde{\rho}(t,u)du \tag{B4}$$

is the integral characterizing the probability for a neuron to remain in the inactive state. According to Eq. (B1), the amplitude $\rho(t)$ decreases due to crossing the threshold T. The shape $p(t,u)$ is renormalized, i.e., it is governed by Eq. (B1) with the added source term proportional to $p(t,u)$ itself, i.e.,

$$\tau_m(t)\frac{\partial p}{\partial t} + \frac{\partial}{\partial u}\left(-up - \frac{1}{2}\frac{\partial p}{\partial u}\right) = \tilde{H}(t)p(t,u), \tag{B5}$$

where $\tilde{H}(t)$ is the activity,

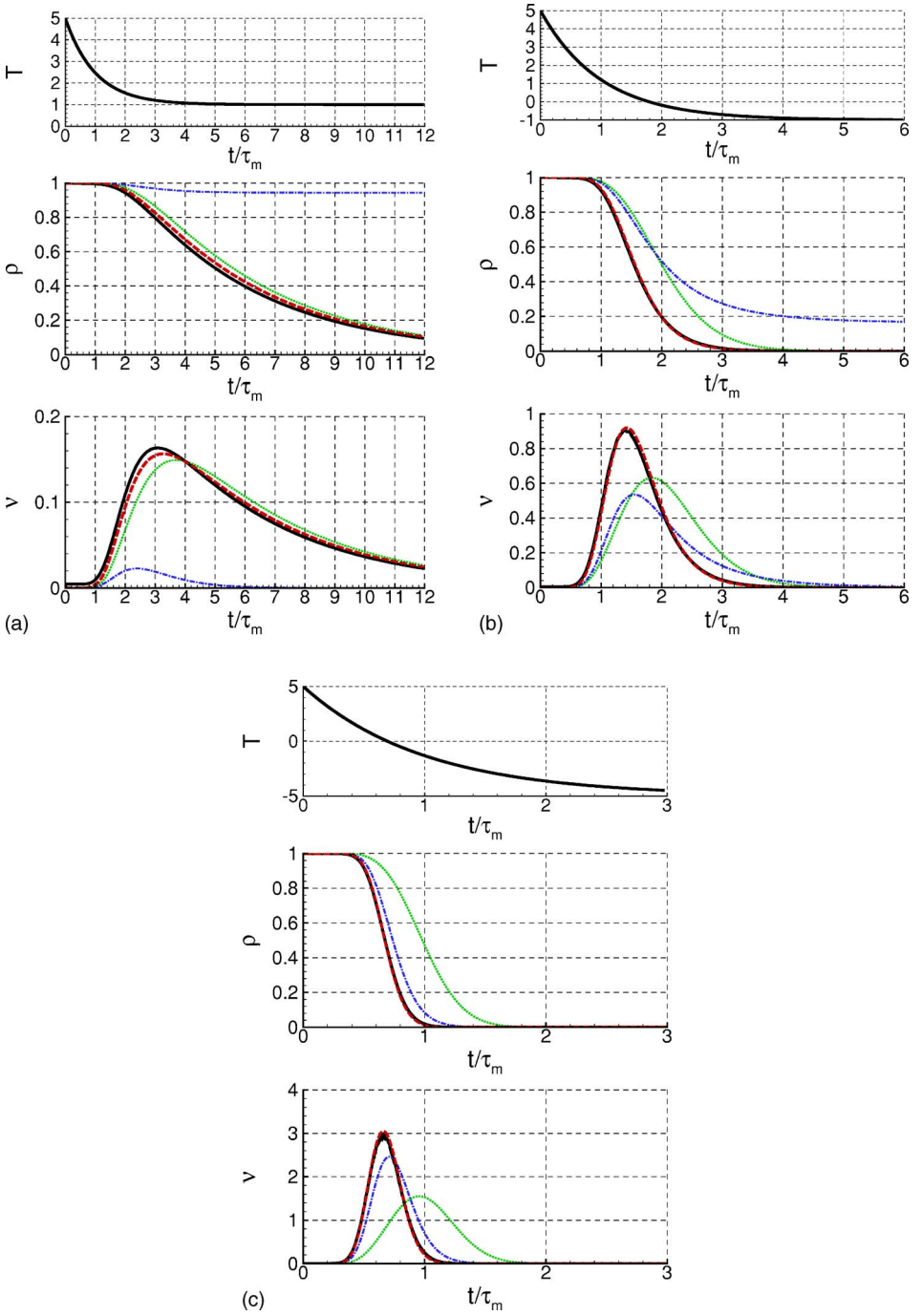

FIG. 11. (Color online) Comparison of the firing rate $\nu(t)=\partial\rho/\partial t$ calculated by the full Fokker-Planck equation (B1) (black solid lines) with the approximations by $\tau_m d\rho/dt=-\rho A(T)$ (green dotted line), $\tau_m d\rho/dt=-\rho B(T,dT/dt)$ (blue dot-dashed line) and $\tau_m d\rho/dt=-\rho(A(T)+B(T,dT/dt))$ (red long-dashed line). The evolution of $T(t)$ is defined by the input $U(t)=U_{max}[1-\exp(-t/\tau_m)]$, $U^T=5\sigma$, corresponding to the current-step stimulation. The subthreshold (a), near-threshold (b), and suprathreshold (c) regimes were set by $U_{max}/\sigma=4$, 6, or 10, respectively.

$$\tilde{H}(t)=\frac{1}{2}\left.\frac{\partial p}{\partial u}\right|_{u=T}. \tag{B6}$$

The boundary conditions are $p(t,T)=0$, $p(t,-\infty)=0$, and the initial condition $p(0,u)=1/\sqrt{\pi}\exp(-u^2)$.

The amplitude of the probability distribution, $\rho(t)$ is described by the equation

$$\tau_m(t)\frac{d\rho}{dt}=-\rho\tilde{H}(t), \tag{B7}$$

and the activity $\tilde{H}(t)$ plays the role of the hazard function in the population model, i.e., $H\equiv\tilde{H}/\tau_m$ for Eq. (9).

1. Self-similar solution

When the potential difference between the mean potential U and the threshold U^T is slowly changing, the diffusion process described by the Fokker-Planck equation prevails over the transfer process. The limit case is when T is constant. The solution of Eq. (B1) in this case is self-similar with decreasing amplitude $\rho(t)$ and constant shape $p(t,u)$, described by the stationary variant of Eq. (B5),

$$\frac{d}{du}\left(-up-\frac{1}{2}\frac{dp}{du}\right)=Ap,\quad A(t)=\frac{1}{2}\left.\frac{\partial p}{\partial u}\right|_{u=T}, \tag{B8}$$

with the same boundary conditions. The solution can be found analytically and expressed by the infinite series described by Kummer's functions. Examples of such solutions are demonstrated in Fig. 10. We are interested in the dependence of the activity, $A \equiv \tilde{H}$, on T, shown in Fig. 5(a).

2. Frozen Gaussian distribution

In the opposite limit case, when $T(t)$ is decreasing rapidly, the initial Gaussian distribution remains almost unchanged except for a cutting off at the threshold $u=T$. The hazard function in this particular case, $B \equiv \tilde{H}$, depends on $T(t)$ and its time derivative dT/dt, i.e., $B=B(T,dT/dt)$. According to Eq. (B7), this function can be derived as

$$B = -\frac{\tau_m}{\rho}\frac{d\rho}{dt}, \tag{B9}$$

where ρ is governed by Eq. (B4).

For simplicity, we consider the case of monotonically increasing but otherwise arbitrary $T(t)$. Substituting the Gaussian distribution $\tilde{\rho}(t,u)=\tilde{\rho}(0,u)$ according to Eq. (B2) into Eq. (B4) and then into Eq. (B9), we obtain

$$B(T,dT/dt) = -\frac{\tau_m}{\rho}\frac{d\rho}{dT}\left[\frac{dT}{dt}\right]_+ = -\tau_m\sqrt{2}\frac{dT}{dt}\tilde{F}(T), \tag{B10}$$

$$\text{where} \quad \tilde{F}(T) = \sqrt{\frac{2}{\pi}}\frac{\exp(-T^2)}{1+\mathrm{erf}(T)}$$

and $[x]_+=x$ for $x>0$ and zero otherwise. The obtained dimensionless function $\tilde{F}$ is shown in Fig. 5(b).

3. Approximation of hazard function in arbitrary case

It is proposed to consider the following approximation of the hazard function:

$$\tilde{H} = A + B \tag{B11}$$

where $A(T)$ is given by Fig. 5(a), and $B(T,dT/dt)$ is given by Eq. (B10).

Comparison of the exact and approximate solutions is shown in Fig. 11. Three cases of neuron stimulation by the injected current steps of three different amplitudes were simulated. As seen, the approximation by Eq. (B11) works well in different regimes of neuron stimulation. In fact, the approximation $\tilde{H}=A$ works well only in the subthreshold stimulation regime and the approximation $\tilde{H}=B$ does well only in the superthreshold stimulation regime, whereas Eq. (B11) gives a good approximation in all three regimes.

APPENDIX C: NUMERICAL METHOD

For numerical integration of the governing equations (9), (11), and (12) we write the numerical scheme. These equations are one-dimensional transport equations of the hyperbolic type, which can be written as follows:

$$\frac{\partial z}{\partial t} + \frac{\partial z}{\partial t^*} = S_z(t,t^*), \tag{C1}$$

where $z=z(t,t^*)$ is one of the functions ρ, U, x, or y; $S_z(t,t^*)$ is the source term corresponding to the right-hand side of the one of these functions.

For this equation we use the finite-difference total variation diminishing scheme [21], which provides the second order of approximation in both directions of the independent coordinates t and t^*, and monotonicity of the solution, i.e., it avoids artificial extremums. The time and the t^* space are discretized with the intervals Δt and Δt^*, respectively. We consider $N-1$ equal intervals in the t^* space and cumulate the rest of the space in the Nth numerical cell. The scheme is written for the nth time step and the ith cell in t^* space as follows:

$$z_i^{n+1} = z_i^n - \frac{\Delta t}{\Delta t^*}\left[z_i^n - z_{i-1}^n + \frac{1}{2}\left(1-\frac{\Delta t}{\Delta t^*}\right)(w_i^z - w_{i-1}^z)\right] + \Delta t(S_z)_i^n \quad \text{for } i=1,\ldots,N-1, \tag{C2}$$

where

$$w_i^z = \lim(z_{i+1}-z_i, z_i - z_{i-1}),$$

$$\lim(a,b) = \begin{cases} 0 & \text{if } ab <= 0; \\ -\min(|a+b|/2, 2\min(|a|,|b|)) & \text{if } a<0,\ ab>0; \\ \min(|a+b|/2, 2\min(|a|,|b|)) & \text{otherwise} \end{cases}$$

with the boundary values $w_0^z=0$, $w_N^z=0$.

The boundary conditions at the left are given in Sec. II C. At the right, to provide neuron number conservation the density in the last (Nth) cell is calculated by

$$\rho_N^{n+1} = \rho_N^n + \frac{\Delta t}{\Delta t^*}\left(\rho_{N-1}^n + \frac{1}{2}\left(1-\frac{\Delta t}{\Delta t^*}\right)w_{N-1}^\rho\right] + \Delta t(S_\rho)_N^n. \tag{C3}$$

The firing rate is calculated as

$$\rho_0^{n+1} = \rho_0^n - \frac{\Delta t}{\Delta t^*}\rho_0^n - \Delta t\sum_{i=1}^{N}(S_\rho)_i^n. \tag{C4}$$

The voltage and the gating variables of ionic currents in the last (Nth) cell are calculated as follows:

$$z_N^{n+1} = z_N^n + \Delta t(S_z)_N^n, \tag{C5}$$

where $z=z(t,t^*)$ is one of the functions U, x, or y.

For the simulations described in Sec. III we used the following values for numerical parameters: $\Delta t=0.1$ ms, $\Delta t^*=0.5$ ms, $N=400$.

[1] B. Knight, J. Gen. Physiol. **59**, 734 (1972).
[2] J. Eggert and J. L. van Hemmen, Neural Comput. **13**, 1923 (2001).
[3] A. Omurtag, B. W. Knight, and L. Sirovich, J. Comput. Neurosci. **8**, 51 (2000).
[4] W. Gerstner and W. M. Kistler, *Spiking Neuron Models, Single Neurons, Populations, Plasticity* (Cambridge University Press, Cambridge, U.K., 2002).
[5] A. V. Chizhov, L. J. Graham, and A. A. Turbin, Neurocomputing **70**, 252 (2006).
[6] P. Dayan and L. F. Abbott, *Theoretical Neuroscience* (MIT Press, Cambridge, MA, 2001).
[7] P. A. Robinson, C. J. Rennie, and J. J. Wright, Phys. Rev. E **56**, 826 (1997).
[8] O. Shriki, D. Hansel, and H. Sompolinsky, Neural Comput. **15**, 1809 (2003).
[9] M. N. Zhadin, Biophysics (Engl. Transl.) **39**, 129 (1994).
[10] A. V. Chizhov, Biophysics (Engl. Transl.) **47**, 1007 (2002).
[11] D. Nykamp and D. Tranchina, J. Comput. Neurosci. **8**, 19 (2000).
[12] L. Borg-Graham, in *Cerebral Cortex*, edited by P. S. Ulinski, E. G. Jones, and A. Peters (Plenum Press, New York, 1999), Vol. 13, pp. 19–138.
[13] N. Kopell, G. B. Ermentrout, M. A. Whittington, and R. D. Traub, Neurobiology **97**, 1867 (2000).
[14] S. Karnup and A. Stelzer, J. Physiol. (London) **516**, 485 (1999).
[15] S. Karnup and A. Stelzer, J. Physiol. (London) **532**, 713 (2001).
[16] P. I. M. Johannesma, *Neural Networks* (Springer, Berlin, 1968), pp. 116–144; also see Eq. (5.104) in [4].
[17] L. F. Abbott and C. van Vreeswijk, Phys. Rev. E **48**, 1483 (1993).
[18] N. Brunel and V. Hakim, Neural Comput. **11**, 1621 (1999).
[19] R. Jolivet, T. J. Lewis, and W. Gerstner, J. Neurophysiol. **92**, 959 (2004).
[20] A. N. Pokrovskii, Biofizika **23**, 649 (1978).
[21] A. Harten and S. Osher, SIAM (Soc. Ind. Appl. Math.) J. Numer. Anal. **24**, 279 (1987).